



Tropopause altitude determination from temperature profiles of reduced altitude resolution

Nils König¹, Peter Braesicke¹, and Thomas von Clarmann¹

¹Karlsruhe Institute of Technology, Institute of Meteorology and Climate Research,
Karlsruhe, Germany

Correspondence: T. von Clarmann (thomas.clarmann@kit.edu)

Abstract. Inference of the lapse rate tropopause or the cold point from temperature profiles of finite vertical resolution entails an uncertainty of the tropopause altitude. For tropical radiosonde profiles the tropopause altitude inferred from coarse grid profiles was found to be lower than that inferred from the original profiles. The mean displacements of the lapse rate tropopause altitude when inferred from a temperature profile of 3 km vertical resolution and a Gaussian kernel is -240 m. In case of a 5 MIPAS averaging kernel the displacement of the lapse rate tropopause altitude is -640 m. The displacement of the cold point tropopause inferred from a temperature profile of 3 km vertical resolution (Gaussian kernels) was found to be -500 m. The spread of the results seems too large as to recommend a correction scheme.

1 Introduction

The tropopause constitutes a vertical separation in the atmosphere that segregates the lower, weather active region, *viz.*, the 10 troposphere, from an upper, steadier region, the stratosphere. High altitude temperature soundings that became possible at the end of the 19th century showed an – at that time – unexpected temperature behaviour, where temperatures would stagnate or even increase with height (see Hoinka, 1997, for a historical overview). Once it was established that this observation was no measurement error, and that above the troposphere another region of the atmosphere exist, namely the stratosphere, an 15 unambiguous definition for the height of the boundary, the tropopause, had to be agreed. The earliest comprehensive definition provided by the British Meteorological Office was based on either the existence of a temperature inversion, or an abrupt transition to a temperature gradient below 2 K/km. If the first two criteria were not met, a more general vertical temperature gradient criterion was applied: “at the point where the mean fall of temperature for the kilometre next above is 2 K or less provided that it does not exceed 2 K for any subsequent kilometre” Dines (1919, cited after Hoinka, 1997). A similar definition, 20 focusing solely on the lapse rate of 2 K/km was adapted by the World Meteorological Organization (WMO) in later years (World Meteorological Organization, 1957). Since then additional definitions of the tropopause have emerged, focusing on the behaviour of dynamical quantities (e.g. Hoerling et al., 1991) or of trace gas changes (e.g. Pan et al., 2004). However, the most commonly used method to define the position of the tropopause still is the WMO criterion.

In tropical latitudes, another useful reference for distinguishing the tropopause from the stratosphere is the cold point (where the temperature minimum occurs). It relates to the existence of a temperature inversion in the original definition as described



above and the corresponding lapse rate tropopause lies commonly a few hundred meters below the cold point (e.g., Figure 8 in Kim and Son, 2012).

Aspirational targets exist for knowing the altitude distribution of the thermal tropopause with an uncertainty of 100 m globally (see the Observing Systems Capability Analysis and Review Tool at <https://www.wmo-sat.info/oscar/variables/view/81>).
5 However, it is obvious that deriving the altitude of a lapse rate tropopause will depend to some extent on the resolution of the temperature profile that is used to calculate the vertical gradient. The same holds true for the cold point tropopause. Thus, it seems important to understand how the derived altitude of the tropopause depends on the vertical resolution of the temperature data. Knowledge of the exact tropopause altitude is essential in particular, when distributions of atmospheric state variables such as mixing ratios of trace species are transformed to a tropopause-related vertical coordinate system in order to investigate
10 chemical, transport and mixing processes in the upper troposphere and lowermost stratosphere.

The goal of this paper is to analyze the possible dependence of a derived tropopause altitude on the vertical resolution of the temperature profile and to evaluate possibilities to potentially correct tropopause altitudes inferred from coarsely resolved temperature profiles. After presenting the formal concept used for this study (Section 2), we first asses the impact of finite vertical resolution on the determination of the tropopause altitude in quantitative terms (Section 3). We do this separately
15 for lapse rate tropopause altitudes (Section 3.1) and cold point tropopause altitudes (Section 3.2). Then, focusing on low latitudes, we investigate if related altitude errors can be corrected by a slight modification of the tropopause definition which, when applied to temperature profiles of finite vertical resolution, reproduces the tropopause altitude according to the WMO definition when applied to the original data (Section 4). Finally we discuss the applicability of our results to various types of constrained temperature retrievals from satellite data (Section 5) and conclude what the upshot of this study is from a data user
20 perspective (Section 6).

2 The formal concept

The altitude resolution of a vertical profile such as temperature can be characterized by the $n \times n$ averaging kernel matrix **A** (Rodgers, 2000). It consists of the partial derivatives $\frac{\partial \tilde{x}_i}{\partial x_j}$ of the elements \tilde{x}_i of the degraded profile with respect to the variation of the element x_j of the true profile. Its columns represent the relative response of a degraded profile \tilde{x} to a delta perturbation
25 of the true profile x . Conversely, the j th column represents the weights with which the elements of the true profile contribute to the j th element of the degraded profile. The averaging kernel of a profile without degradation is the identity matrix **I**. It goes without saying that effects on a finer scale than that reproducible in the n -dimensional grid remain undetected, unless some prior information on the profile shape between the gridpoints is used, as suggested by, e.g., Reichler et al. (2003). This is to say, the averaging kernel does not characterize the degradation with respect to the fully resolved true profile but only the
30 degradation with respect to the profile represented in a vector of n gridpoints.

Typically, the reduction of altitude resolution is caused by one of the following three mechanisms: (1) the atmosphere is remotely sensed by an instrument of finite vertical resolution. In this case, the atmospheric state is often sampled on a grid finer than that corresponding to the altitude resolution of the measurement system; (2) A high-resolution profile is resampled on a



coarser grid. This resampling goes along with a degradation of the altitude resolution; (3) a filter function is applied, which reduces the vertical resolution.

2.1 Remotely sensed vertical profiles

Often the degradation, i.e., the loss of vertical resolution, is caused by the use of a constraint in the retrieval of atmospheric
 5 state variables from remote measurements \mathbf{y} . The estimated state $\hat{\mathbf{x}}$ depends on the measurement \mathbf{y} and the prior information \mathbf{x}_a as

$$\hat{\mathbf{x}} = \mathbf{x}_a + (\mathbf{K}^T \mathbf{S}_y^{-1} \mathbf{K} + \mathbf{R})^{-1} \mathbf{K}^T \mathbf{S}_y^{-1} (\mathbf{y} - \mathbf{f}(\mathbf{x}_a)) \quad (1)$$

where \mathbf{K} is the Jacobian matrix $\frac{\partial y_i}{\partial x_j}$, T indicates a transposed matrix, \mathbf{S}_y is the covariance matrix characterizing measurement noise, \mathbf{R} is a regularization matrix, and \mathbf{f} is the radiative transfer function (von Clarmann et al., 2003a). Using an inverse a
 10 priori covariance matrix \mathbf{S}_a^{-1} as regularization matrix, this formalism renders a maximum a posteriori retrieval as described by Rodgers (2000). Other widely used choices of \mathbf{R} are squared l th order difference matrices (see, e.g. von Clarmann et al., 2003b). The latter are often used in order to stabilize the profile by smoothing without pushing the values towards an a priori profile (e.g. Steck and von Clarmann, 2001).

In all cases, the averaging kernel matrix is

$$15 \quad \mathbf{A}_{\text{retrieval}} = (\mathbf{K}^T \mathbf{S}_y^{-1} \mathbf{K} + \mathbf{R})^{-1} \mathbf{K}^T \mathbf{S}_y^{-1} \mathbf{K}, \quad (2)$$

and with this the state estimate can be separated into two components, which are the contribution of the true atmospheric state and the contribution of the prior information

$$\begin{aligned} \hat{\mathbf{x}} = & \mathbf{A}_{\text{retrieval}} \mathbf{x}_{\text{true}} \\ & + (\mathbf{I} - \mathbf{A}_{\text{retrieval}}) \mathbf{x}_a + \epsilon_{x; \text{total}} \end{aligned} \quad (3)$$

20 where, as its index suggests, \mathbf{x}_{true} represents the true temperature profile, and $\epsilon_{x; \text{total}}$ is the actual realization of the retrieval error.

The altitude resolution of the retrieval can be determined from the averaging kernel matrix. Common conventions are to either use the halfwidths of its rows or the gridwidths divided by the diagonal elements. It goes without saying that the altitude resolution of a retrieved profile can be altitude-dependent.

25 2.2 Resampling on a coarser grid

Other causes for degraded profiles are representation on a grid not sufficiently fine to represent all structures or application of a numerical filter to the original profile. The averaging kernel matrix is the adequate tool for dealing with all these cases.

The effect of a coarse grid is best understood by construing the coarse-grid profile as a result of an interpolation of the profile from a finer grid (see Rodgers 2000, Sect 10.3.1, where a slightly different notation is used). Let $\tilde{\mathbf{x}}$ be the profile represented



on the coarse grid, and \tilde{x} the profile in the original representation where all fine structure is resolved. In this case we use an interpolation matrix \mathbf{V} and get

$$\tilde{x} = \mathbf{V}x \quad (4)$$

For an interpolation from a fine grid to a coarse grid \mathbf{V} is often chosen as

$$5 \quad \mathbf{V} = (\mathbf{W}^T \mathbf{W})^{-1} \mathbf{W}^T, \quad (5)$$

where \mathbf{W} is the interpolation from the coarse to the fine grid. A definition of \mathbf{A} based on \mathbf{V} gives us an asymmetric averaging kernel matrix which represents the dependence of the profile values on the coarse grid on the “true” values on the fine grid.

$$\mathbf{A}_{\text{coarse}} = \mathbf{V} \quad (6)$$

Contrary to the averaging kernel matrix introduced by Eq (2), $\mathbf{A}_{\text{coarse}}$ is not quadratic.

10 To characterize the loss of resolution due to coarse sampling the averaging kernel on the fine grid, $\mathbf{A}_{\text{interpolation}}$, is needed. It is

$$\mathbf{A}_{\text{interpolation}} = \mathbf{W} \mathbf{V}. \quad (7)$$

If the profile on the fine grid is in itself a degraded profile, e.g., because it was generated by a constrained retrieval, we need a combined averaging kernel matrix

$$15 \quad \mathbf{A}_{\text{combined}} = \mathbf{W} \mathbf{V} \mathbf{A}_{\text{retrieval}}. \quad (8)$$

2.3 Application of filter functions

Application of a linear filter corresponds to the convolution of the original profile with a filter function and is best formulated as a matrix product involving a filter matrix \mathbf{T} whose lines correspond to the moving discretized filter functions at its actual position.

$$20 \quad \tilde{x} = \mathbf{T}x \quad (9)$$

In this case the averaging kernel matrix is identical to the \mathbf{T} matrix.

$$\mathbf{A}_{\text{filter}} = \mathbf{T} \quad (10)$$

3 The dependence of the estimated tropopause altitude on vertical resolution of the underlying temperature profile

To analyze the impact of smoothing effects on the estimated tropopause altitude we use temperature profiles measured by 25 radiosondes launched from Nairobi, 1.21°S 36.8°E. These data were available via the Southern Hemisphere Additional



Table 1. Radiosonde launches from Nairobi

Date of Radiosonde Launches			
09-06-2010	15-06-2010	23-06-2010	30-06-2010
07-07-2010	14-07-2010	21-07-2010	28-07-2010
03-08-2010	11-08-2010	18-08-2010	25-08-2010
08-09-2010	15-09-2010	23-09-2010	29-09-2010
06-10-2010	13-10-2010	19-10-2010	27-10-2010
03-11-2010	10-11-2010	17-11-2010	24-11-2010
01-12-2010	08-12-2010	15-12-2010	22-10-2010
29-12-2010			

Ozonesondes (SHADOZ) network (<https://tropo.gsfc.nasa.gov/shadoz/>, retrieved on 20 May 2017, Witte et al. 2017; Thompson et al. 2017). Details of the sonde profiles used in our study are compiled in Table 1. We focus on tropical temperature profiles, because of the importance of the tropical tropopause in the climate system. Obviously, the area of the tropics exceeds that of other latitude bands; the tropical tropopause is the entry point of air into the stratosphere (Fueglistaler et al., 2009); and 5 finally the tropical tropopause region plays a distinctive role in the radiative budget of the Earth (Riese et al., 2012).

Various averaging kernels \mathbf{A} are applied to the original radiosonde profiles \mathbf{x} to get degraded temperature profiles $\tilde{\mathbf{x}}$. These are used for determination of the lapse rate tropopause altitude and the results are then compared to the tropopause altitudes determined from the original sonde data.

3.1 The Lapse Rate Tropopause

10 The lapse rate tropopause is the lower boundary of the lowermost layer where the temperature gradient is larger (more positive) than -2 K/km provided that the average lapse rate between this level and all higher levels within 2 km does not exceed 2 K/km (World Meteorological Organization, 1992). It is often determined from data resampled on a grid corresponding to a wider range of vertical spacings from below 1 km (e.g., significant pressure levels) and not always from the raw radiosonde data (see, e.g., Reichler et al. 2003, and references therein).

15 From the radiosonde profiles the lapse rate tropopause altitudes were determined and served as our benchmark. In subsequent steps, the profiles were systematically degraded using averaging kernels of different shapes and altitude resolutions, in order to investigate a possible vertical displacement of the apparent tropopause.

3.1.1 Gaussian averaging kernels

In a first test series we use Gaussian-shaped averaging kernels to smooth the original radiosonde profiles. For this purpose we 20 use the radiosonde data on their native grid. The smoothed profiles are sampled on a 1-km altitude grid. Half widths (Full width at half maximum) of 1 to 5 km were tested. Since we are not interested in the contribution by any a priori profile but only in the

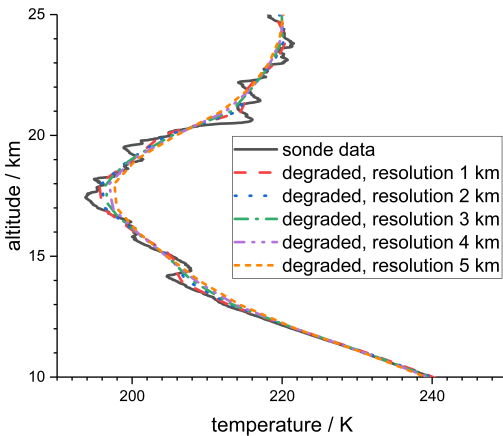


Figure 1. A radiosonde temperature profile measured at Nairobi, 1.21°S 36.8°E on 18 August 2010, 7:35 UT, along with a set of degraded profiles (Gaussian kernel) with resolutions of from 1 to 5 km.

degradation of the vertical profiles by a degraded altitude resolution, we use Eq. (9), with the necessary modification to cope with the irregular input grid.

An example of an original radiosonde profile and a set of smoothed profiles are shown in Figure 1. These smoothed profiles were used to determine the tropopause altitudes according to the lapse rate criterion. Histograms of resulting vertical tropopause 5 displacements for all profiles listed in Table 1 are shown in Figures 2. They are well-behaved in a sense that they have no pronounced secondary modes and are fairly symmetric. Apparent asymmetries are caused by the wide bins which are necessary to have enough data points per bin.

The average tropopause displacement as a function of vertical resolution is shown in Fig. 3. Tropopause altitudes inferred from coarser reduced data tend to be lower than those determined from the original sonde data. For a resolution of 3 km the 10 mean (median) tropopause altitude displacement was found to be -240 m (-110 m). The median is less affected than the mean at all resolutions. The 5 to 95 percentile range increases for coarser resolutions and reaches saturation at a resolution beyond 3 km.

3.1.2 MIPAS averaging kernels

The Michelson Interferometer for Passive Atmospheric Sounding (MIPAS, Fischer et al. 2008) was an infrared limb emission 15 spectrometer operating on the Envisat research satellite. One of its data products was global temperature distributions from the upper troposphere to the mesosphere (von Clarmann et al., 2003b, 2009). We complement the theoretical study presented above with an assessment of how MIPAS temperature averaging kernels affect the lapse rate tropopause determination. For this purpose we use averaging kernels and the a priori of MIPAS retrievals which are spatiotemporally as close as possible to the

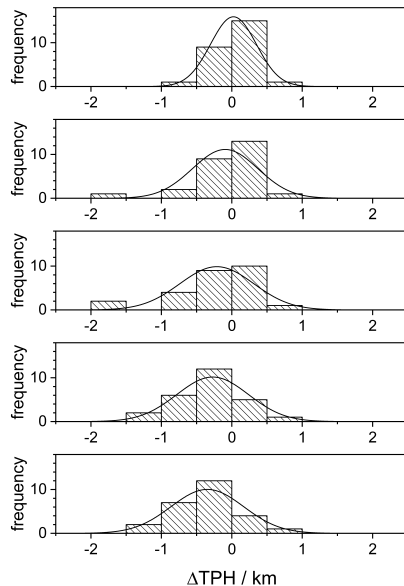


Figure 2. Histograms and mean tropopause height (TPH) offsets of degraded temperature profiles (Gaussian kernel) with resolutions of 1 to 5 km in steps of 1 km (from top to bottom). Note that the apparent asymmetry of some of the histograms is accentuated by the symmetric choice of relatively large bins to accomodate a reasonable amount of results per bin.

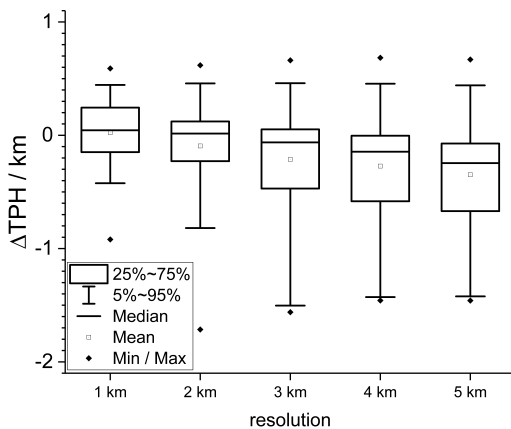


Figure 3. The lapse rate tropopause displacement as a function vertical resolution for Gaussian kernels. Boxes represent both of the second and the third quartile. The “error bars” represent the central 90% quantile.



Table 2. MIPAS collocations

Date	Time (UTC)
09-06-2010	08:08:53
14-07-2010	08:08:54
03-08-2010	07:40:09
23-09-2010	07:37:27
28-10-2010	19:46:35
24-11-2010	19:58:09
08-12-2010	19:44:25

radiosonde measurements (Table 2). The MIPAS geolocations deviate from that of the Nairobi radiosonde launch site by less than $\pm 5^\circ$ in latitude and less than $\pm 10^\circ$ in longitude.

Since MIPAS averaging kernels are provided on a 1-km altitude grid, we use the radiosonde profiles resampled on a 1-km vertical grid, using Equation (6) with a \mathbf{V} matrix for linear interpolation. Since the MIPAS averaging kernels ($\mathbf{A}_{\text{MIPAS}}$) are 5 routinely produced on a 1-km grid (see, Fig. 4 for an example), they can then be conveniently applied to these resampled radiosonde profiles. The application of the averaging kernels as a filter function given by

$$\mathbf{x}_{\text{degraded}} = \mathbf{A}_{\text{MIPAS}} \mathbf{x}_{\text{radiosonde}} \quad (11)$$

yields the radiosonde profile at the vertical resolution of the MIPAS temperatures. It does, however, not include the contribution of the a priori profiles used in the MIPAS retrieval. A more realistic transformation, which provides the radiosonde profiles as 10 MIPAS would see them, involves Eq. (3). Its application to the problem under investigation reads

$$\begin{aligned} \mathbf{x}_{\text{degraded}} &= \mathbf{A}_{\text{MIPAS}} \mathbf{x}_{\text{radiosonde}} \\ &+ (\mathbf{I} - \mathbf{A}_{\text{MIPAS}}) \mathbf{x}_{\text{ERA-Interim}}, \end{aligned} \quad (12)$$

where $\mathbf{x}_{\text{ERA-Interim}}$ are temperature profiles extracted from ECMWF ERA-Interim analyses (Dee et al., 2011), which were used as a priori information for the MIPAS retrievals. Since actual MIPAS measurement data are not used directly but only for 15 the calculation of the averaging kernels, the noise term is not considered here.

The resulting profile $\mathbf{x}_{\text{degraded}}$ is the radiosonde profile as MIPAS would have seen it, if it had made a noise-free measurement exactly at the place and time of the radiosonde measurements. Again, the effect of the reduced resolution, now along with the effect of the a priori temperature profiles, on the tropopause altitude determination is investigated (Fig. 5). The mean tropopause altitude offset is -640 m; the median is -530 m. The sign of these results are consistent with those obtained for 20 Gaussian kernels. The displacement, however, is considerably larger for the MIPAS averaging kernels.

The consideration of the prior information used is important. The reason is roughly this. In remote sensing applications, instead of referring to the resulting profile, the altitude resolution refers to the difference between the resulting profile and the a priori profile. The fine structure of the prior information is propagated into the resulting profile retrieval and only corrections on a larger scale are founded on the MIPAS measurements.

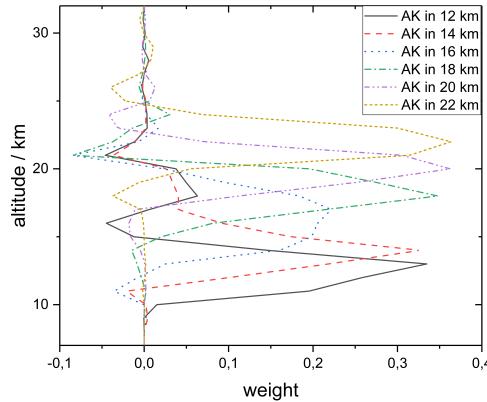


Figure 4. Averaging kernels of a MIPAS measurement near Nairobi on 3 August 2010. The MIPAS altitude resolution is altitude dependent and varies between 2.7 and 4.5 km below 22 km altitude, with typical values around 3.0 km. To avoid an overly busy plot, only every other averaging kernel is shown.

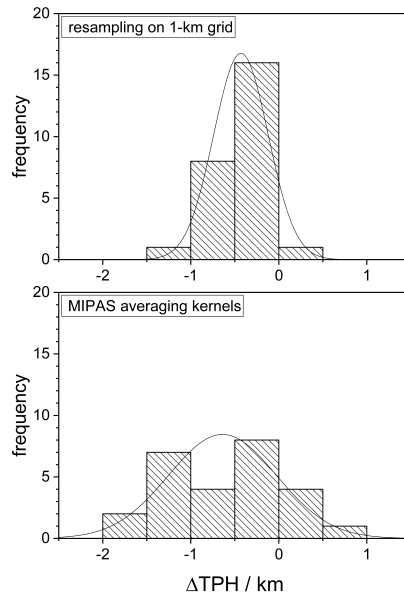


Figure 5. Histogram of tropopause altitude offsets for degraded temperature profiles. The top panel shows the tropopause height displacement by resampling the original sonde data on a regular 1-km grid (Eqs. (5) and (6)). The lower panel shows the effect of the MIPAS averaging kernels according to Eq. (12).

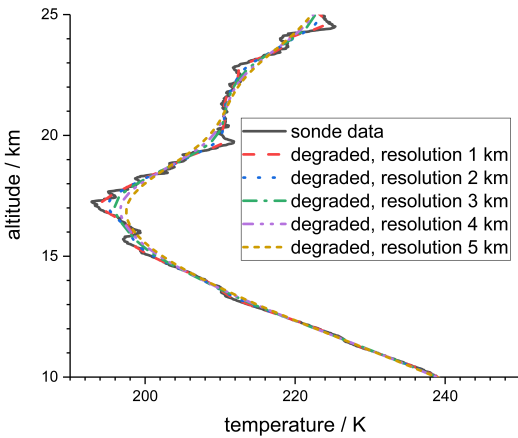


Figure 6. An example of a radiosonde profile, Nairobi, 1.21°S 36.8°E , 7 July 2010, at original vertical resolution along with degraded profiles at vertical resolutions of 1 to 5 km.

In Equation (12) errors in MIPAS and radiosonde data and, more important in this context, spatio-temporal mismatch between the MIPAS and the radiosonde measurements are neglected. The latter is particularly problematic. According to Equation (12) the atmosphere as seen by MIPAS contains a priori information, which is in this case the ERA-Interim temperature profile at the MIPAS measurement location. Any tropopause altitude difference between the MIPAS time and measurement 5 location and the radiosonde time and measurement location can hardly be distinguished from the tropopause altitude offset caused by the degraded vertical resolution.

3.2 The Cold Point Tropopause

In addition to the sensitivity of the lapse rate tropopause altitude to the vertical resolution of the temperature profile, also cold point tropopause altitudes were investigated. Again Gaussian averaging kernels were assessed (Fig 6).

10 Here, the degrading with the Gaussian kernel was performed directly to the radiosonde profiles on their original grids and the cold point tropopauses were determined. The dependence of the cold point tropopause altitude on the vertical resolution is shown in Fig. 7.

15 Also the cold point tropopause altitudes inferred from coarser resolved temperature profiles are lower than those inferred from the original profiles. We assume that the Nairobi profiles are representative of the tropical atmosphere. However, we note that these results might not be applicable for other latitude bands. With -500 m (430 m) the mean (median) tropopause altitude displacement exceeds that of the lapse rate tropopause by far.

MIPAS data are sampled on a 1-km grid, and data of satellite instruments of similar vertical resolution are typically sampled on even coarser grids. Determination of the cold point tropopause on such a grid would thus by far be dominated by sampling effects. Tropopause shifts of a magnitude as determined with the Gaussian kernel thus cannot be resolved.

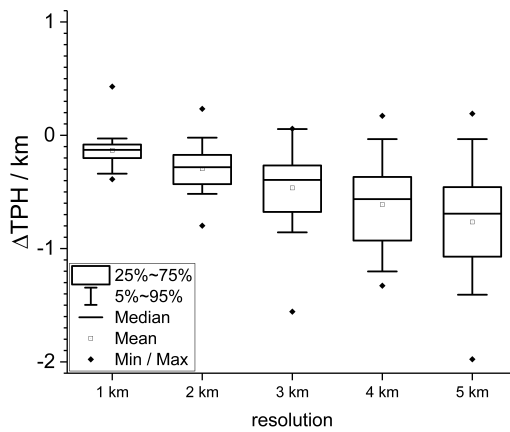


Figure 7. The cold point tropopause displacement as a function of the vertical resolution for Gaussian kernels. For details, see Fig. 3.

4 Feasibility of Correction Schemes

Since degraded, i.e., less resolved, temperature profiles are thought to exhibit less steep gradients, it suggests itself to adjust the lapse rate threshold in the WMO definition of the tropopause to compensate the smoothing effect. Doing this, one might expect to find the tropopause at the correct altitude even from degraded profiles. Obviously, the threshold, if any useful, must 5 be a function of the vertical resolution of the temperature profile used.

We have searched for a temperature gradient that, when applied to the coarse resolution profiles, reproduces the same tropopause altitude as the -2 K/km gradient applied to the original profiles. Fig. 8 shows histograms of the obtained adjusted lapse rate criteria for vertical resolutions of 1 to 5 km. There is a tendency that lapse rates between -1 and -2 K/km are more adequate for applications to coarsely resolved profiles but the spread is very large. Therefore, we cannot recommend a general 10 correction scheme.

5 Discussion

Given the variety of retrieval schemes used to infer temperature profiles from satellite measurements, the following caveats with respects to the generality of our results need to be discussed.

Often satellite retrievals use a retrieval scheme similar to Eq. (1) along with a highly structured a priori profile x_a . A retrieval 15 with a vertical resolution which is significantly coarser than that of x_a will modify only the coarse structure of the temperature profile, while the fine structure of the x_a will survive the retrieval process. This is because the resolution of the retrieval as defined by the averaging kernel refers, rigorously speaking, not to the resulting profile, but to the difference between the resulting profile and the a priori profile. Related effects on the tropopause displacement are then complicated to predict.

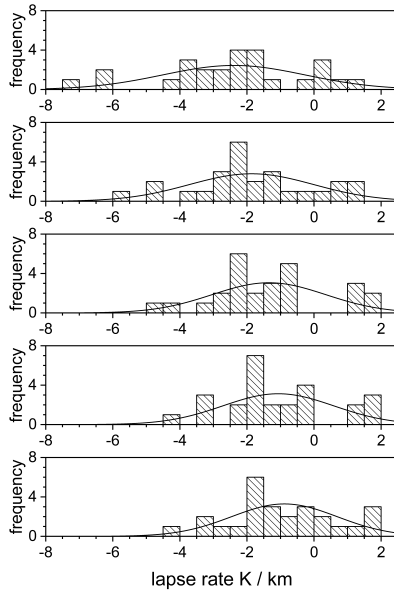


Figure 8. Histograms of optimal lapse rates for tropopause determination from coarsely resolved temperature profiles, along with fitted Gaussian distributions. Vertical resolutions vary from 1 km (top) to 5 km (bottom).

It is the exception rather than the rule that limb sounders use a retrieval grid which is about a factor of three finer than the vertical resolution, as the MIPAS dataset used here. More often the vertical grid is close to the vertical resolution of the retrieval. In these cases, the tropopause altitude determination is limited directly by the sampling of the retrieval and not by its resolution.

5 We focused our investigation on the tropical region. Temperature profiles in other latitude bands can deviate significantly in shape and magnitude, particularly near the tropopause. For midlatitudinal temperature profiles with weak or non-existent gradients above the tropopause even a coldpoint displacement of opposite sign than found here could be possible.

6 Conclusions

In the tropical region the determination of both, the lapse rate and the cold point tropopause altitude from temperature profiles 10 of degraded altitude resolution, typically leads to an underestimation of the tropopause height. The order of magnitude of this effect is in the range of -100 to -500 m for altitude resolutions of 1 to 5 km. This effect is approximately twice as large for the cold point tropopause than for the lapse rate tropopause. This suggests that, while in the tropics the cold point tropopause is commonly used, in the case of coarsely resolved profiles, the lapse rate tropopause appears to be more robust. The variability 15 of this dislocation is fairly large such that recommendation of an inductively generalized correction scheme seems audacious and even inappropriate to us.



Data availability. Radiosonde data were obtained from the SHADOZ website: <https://tropo.gsfc.nasa.gov/shadoz/>. MIPAS data are available via <https://www.imk-asf.kit.edu/english/308.php>.

Competing interests. TvC is associate editor of AMT but has not been involved in the evaluation of this paper.



References

Dee, D. P., Uppala, S. M., Simmons, A. J., Berrisford, P., Poli, P., Kobayashi, S., Andrae, U., Balmaseda, M. A., Balsamo, G., Bauer, P., Bechtold, P., Beljaars, A. C. M., van de Berg, L., Bidlot, J., Bormann, N., Delsol, C., Dragani, R., Fuentes, M., Geer, A. J., Haimberger, L., Healy, S. B., Hersbach, H., Hólm, E. V., Isaksen, L., Kållberg, P., Köhler, M., Matricardi, M., McNally, A. P., Monge-Sanz, B. M., Morcrette, J.-J., Park, B.-K., Peubey, C., de Rosnay, P., Tavolato, C., Thiépaut, J.-N., and Vitart, F.: The ERA-Interim reanalysis: configuration and performance of the data assimilation system, *Q. J. R. Meteorol. Soc.*, 137, 553–597, <https://doi.org/10.1002/qj.828>, 2011.

Dines, W. H.: The characteristics of the free atmosphere, in: *Geophysical Memoirs*, 13, pp. 47–76, Meteorological Office, London, 1919.

Fischer, H., Birk, M., Blom, C., Carli, B., Carlotti, M., von Clarmann, T., Delbouille, L., Dudhia, A., Ehhalt, D., Endemann, M., Flaud, J. M., Gessner, R., Kleinert, A., Koopmann, R., Langen, J., López-Puertas, M., Mosner, P., Nett, H., Oelhaf, H., Perron, G., Remedios, J., Ridolfi, M., Stiller, G., and Zander, R.: MIPAS: an instrument for atmospheric and climate research, *Atmos. Chem. Phys.*, 8, 2151–2188, <https://doi.org/10.5194/acp-8-2151-2008>, 2008.

Fueglistaler, S., Dessler, A. E., Dunkerton, T. J., Folkins, I., Fu, Q., and Mote, P. W.: Tropical Tropopause Layer, *Rev. Geophys.*, 47, RG1004, <https://doi.org/10.1029/2008RG000267>, 2009.

Hoerling, M. P., Schaack, T. K., and Lenzen, A. J.: Global objective tropopause analysis, *Mon. Wea. Rev.*, 119, 1816–1831, 1991.

Hoinka, K. P.: The Tropopause: Discovery, Definition and Demarcation, *Meteorologische Zeitschrift*, 6, 281–303, <https://doi.org/10.1127/metz/6/1997/281>, 1997.

Kim, J. and Son, S.-W.: Tropical Cold-Point Tropopause: Climatology, Seasonal Cycle, and Intraseasonal Variability Derived from COSMIC GPS Radio Occultation Measurements, *J. Clim.*, 25, 5343–5360, <https://doi.org/JCLI-D-11-00554.1>, 2012.

Pan, L. L., Randel, W. J., Gary, B. L., Mahoney, M. J., and Hintsa, E. J.: Definitions and sharpness of the extratropical tropopause: A trace gas perspective, *J. Geophys. Res.*, 109, D23103, <https://doi.org/10.1029/2004JD004982>, 2004.

Reichler, T., Dameris, M., and Sausen, R.: Determining the tropopause height from gridded data, *Geophys. Res. Lett.*, 30, 2042, <https://doi.org/10.1029/2003GL018240>, 2003.

Riese, M., Ploeger, F., Rap, A., Vogel, B., Konopka, P., Dameris, M., and Forster, P.: Impact of uncertainties of atmospheric mixing on simulated UTLS composition and related radiative effects, *J. Geophys. Res.*, 117, D16305, <https://doi.org/10.1029/2012JD017751>, 2012.

Rodgers, C. D.: *Inverse Methods for Atmospheric Sounding: Theory and Practice*, vol. 2 of *Series on Atmospheric, Oceanic and Planetary Physics*, F. W. Taylor, ed., World Scientific, Singapore, New Jersey, London, Hong Kong, 2000.

Steck, T. and von Clarmann, T.: Constrained profile retrieval applied to the observation mode of the Michelson Interferometer for Passive Atmospheric Sounding, *Appl. Opt.*, 40, 3559–3571, 2001.

Thompson, A. M., Witte, J. C., Sterling, C., Jordan, A., Johnson, B. J., Oltmans, S. J., Fujiwara, M., Vömel, H., Allaart, M., Piters, A., Coetzee, G. J. R., Posny, F., Corrales, E., Diaz, J. A., Félix, C., Komala, N., Lai, N., Nguyen, H. T. A., Maata, M., Mani, F., Zainal, Z., Ogino, S., Paredes, F., Penha, T. L. B., da Silva, F. R., Sallons-Mitro, S., Selkirk, H. B., Schmidlin, F. J., Stübi, R., and Thiongo, K.: First reprocessing of Southern Hemisphere Additional Ozonesondes (SHADOZ) ozone profiles (1998–2016): 2. Comparisons with satellites and ground-based instruments, *J. Geophys. Res. Atmos.*, 122, 13,000–13,025, <https://doi.org/10.1002/2017JD027406>, 2017.

von Clarmann, T., Ceccherini, S., Doicu, A., Dudhia, A., Funke, B., Grabowski, U., Hilgers, S., Jay, V., Linden, A., López-Puertas, M., Martín-Torres, F.-J., Payne, V., Reburn, J., Ridolfi, M., Schreier, F., Schwarz, G., Siddans, R., and Steck, T.: A blind test retrieval experiment for infrared limb emission spectrometry, *J. Geophys. Res.*, 108, 4746, <https://doi.org/10.1029/2003JD003835>, 2003a.



von Clarmann, T., Glatthor, N., Grabowski, U., Höpfner, M., Kellmann, S., Kiefer, M., Linden, A., Mengistu Tsidu, G., Milz, M., Steck, T., Stiller, G. P., Wang, D. Y., Fischer, H., Funke, B., Gil-López, S., and López-Puertas, M.: Retrieval of temperature and tangent altitude pointing from limb emission spectra recorded from space by the Michelson Interferometer for Passive Atmospheric Sounding (MIPAS), *J. Geophys. Res.*, 108, 4736, <https://doi.org/10.1029/2003JD003602>, 2003b.

5 von Clarmann, T., Höpfner, M., Kellmann, S., Linden, A., Chauhan, S., Funke, B., Grabowski, U., Glatthor, N., Kiefer, M., Schieferdecker, T., Stiller, G. P., and Versick, S.: Retrieval of temperature, H₂O, O₃, HNO₃, CH₄, N₂O, ClONO₂ and ClO from MIPAS reduced resolution nominal mode limb emission measurements, *Atmos. Meas. Techn.*, 2, 159–175, <https://doi.org/10.5194/amt-2-159-2009>, 2009.

10 Witte, J. C., Thompson, A. M., Smit, H. G. J., Fujiwara, M., Posny, F., Coetzee, G. J. R., Northam, E. T., Johnson, B. J., Sterling, C. W., Mohamad, M., Ogino, S.-Y., Jordan, A., and da Silva, F. R.: First reprocessing of Southern Hemisphere ADditional OZonesondes (SHADOZ) profile records (1998–2015): 1. Methodology and evaluation, *J. Geophys. Res. Atmos.*, 122, 6611–6636, <https://doi.org/10.1002/2016JD026403>, 2017.

World Meteorological Organization: Definition of the tropopause, *Bulletin of the World Meteorological Organization*, 6, 136–137, 1957.

World Meteorological Organization: International Meteorological Vocabulary, Secretariat of the World Meteorological Organization, Geneve, 2nd edn., 1992.